

# Soft Gripping System for Space Exploration Legged Robots

Arthur Candalo<sup>1</sup>, Malik-Manel Hashim<sup>1</sup>, Brigid Hickey<sup>1</sup>, Mickael Laine<sup>1</sup>,  
Mitch Hunter-Scullion<sup>2</sup>, and Kazuya Yoshida<sup>1</sup>

<sup>1</sup> Space Robotics Lab., Tohoku University, Sendai 980-8579, Japan,  
acandalot@dc.tohoku.ac.jp,

<sup>2</sup> Asteroid Mining Corporation Ltd., London E14 9HQ, United Kingdom.

**Abstract.** Although wheeled robots have been predominant for planetary exploration, their geometry limits their capabilities when traveling over steep slopes, through rocky terrains, and in microgravity. Legged robots equipped with grippers are a viable alternative to overcome these obstacles. This paper proposes a gripping system that can provide legged space-explorer robots a reliable anchor on uneven rocky terrain. This gripper provides the benefits of soft gripping technology by using segmented tendon-driven fingers to adapt to the target shape, and creates a strong adhesion to rocky surfaces with the help of microspines. The gripping performances are showcased, and multiple experiments demonstrate the impact of the pulling angle, target shape, spine configuration, and actuation power on the performances. The results show that the proposed gripper can be a suitable solution for advanced space exploration, including climbing, lunar caves, or exploration of the surface of asteroids.

**Keywords:** Soft gripper, Climbing robots, Asteroid exploration, Microspine gripper

## 1 Introduction

The discovery and exploitation of critical resources present in space is now being proposed as one of the most viable solutions to facilitate future space development [1]. To do so, the development of highly capable autonomous robots to navigate and operate freely on planetary and asteroid surfaces is required [2]. Hexapods, and more generally walking robots, will be necessary as they offer stable locomotion, leg versatility, and endurance [3] to perform specific tasks in space.

Thanks to the success of the Hayabusa missions by JAXA, the surface of the asteroids Itokawa and Ryugu (Fig. 1a) are now known to be composed of many random-shaped and extremely uneven rocks.

### 1.1 SCAR-E robot

The presented gripping system has been developed to equip 1R [4] class legged robots such as SCAR-E (Fig. 1b). SCAR-E is an omnidirectional hexapod robot

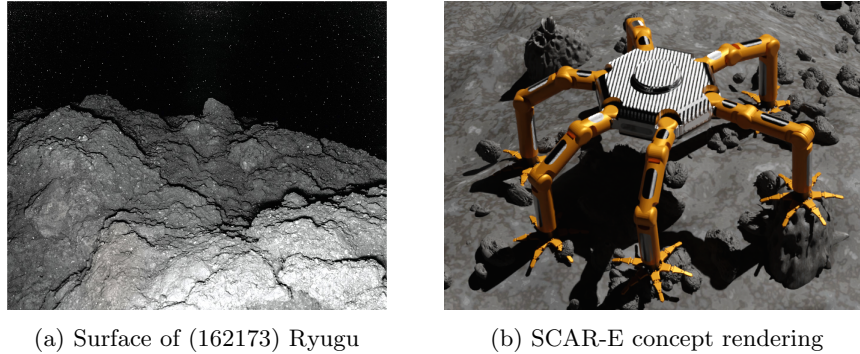


Fig. 1: Asteroid mining prospect for the SCAR-E robot

prototype designed for terrestrial and space applications. It has been designed to perform horizontal and vertical locomotion in uneven environments. The total span of the robot is 1.6 m for 20 kg. The end effector of each leg can be interchanged between a simple foot for basic walking, a gripping system for grasping and climbing or a tool adapted to the specific task at hand. These tools can be combined to create the optimal configuration for the task.

## 1.2 Gripping system for space robots

To overcome the disadvantages of wheeled rovers, legged robots designed for space exploration need to be equipped with efficient grippers that will allow them to climb extreme terrains. The main targets for the use of legged robots in space exploration are rocky terrains such as lava tubes on the Moon [5] or the surface of asteroids. In both cases, the gripper must be reliable and provide a stable anchor point to the ground. To do so, microspines were used to hook the asperities of rocky targets and concentric tangential forces were applied to secure the gripper to the target. Several microspine gripping mechanisms have been developed, such as Parness's LEMUR-II gripper [6], Nagaoka's passive spine gripper [7], or Li's microspine gripper [8]. Although the geometry of the microspine offers some degree of compliance with the target shape, the fixed structure of the finger does not provide adaptability to variations in the range of 1 to 10 cm and is limited to rather flat surfaces. This was observed by Newill-Smith et al. who proposed the use of a multiphalanx gripper for asteroid exploration [9].

## 1.3 Soft-gripping technology

Soft-gripping is an emerging field of research in the world of robotics. Using compliant or deformable fingers actuated with pneumatic [10], tethers [11, 12], or mechanical systems [13], a robot can grasp objects of different sizes, shapes, materials, and textures. The goal of soft-gripping is to maximize the contact surface between the fingers and the targets to apply controlled pressure and

maintain the grasping action with maximal friction. The friction force applied to the target can also be improved by using adhesives [14], or engineering materials similar to the skin of a gecko finger [15]. Other approaches include the use of vacuum-actuated granular pouches to create perfect match contact with the target object [16, 17]. Although these technologies show promising results in the efficient grasp of random-shaped targets, they are limited by extreme temperature changes, a harsh and dusty environment, as well as payload and volume constraints[18]. This research proposes a soft gripping solution that uses microspines and compliant fingers to apply tangential forces and pressure on the target to allow climbing and object manipulation in space.

## 2 Gripping system

The main advantage of soft-gripping technologies is the versatility of the fingers to conform to the shape of its designated target while grasping. This maximizes the contact surface and increases the resulting gripping force. In space environments, polymers and engineered materials are subject to changes in properties as a result of extreme temperature variances, and compliance may not be ensured. For this reason, the proposed gripper is designed with purely mechanical compliance and actuation. To further improve the gripping performance, additional degrees of freedom have been added to each finger for better adaptability. This also allows the gripper to apply a tangential force to the surface of the target and increase the hooking action of the spines onto the porous surface of rocks. A gripper prototype (2) was built using carbon-fiber infused nylon 3D printed parts and stainless steel spines, for a total mass measured at 0.565 kg.

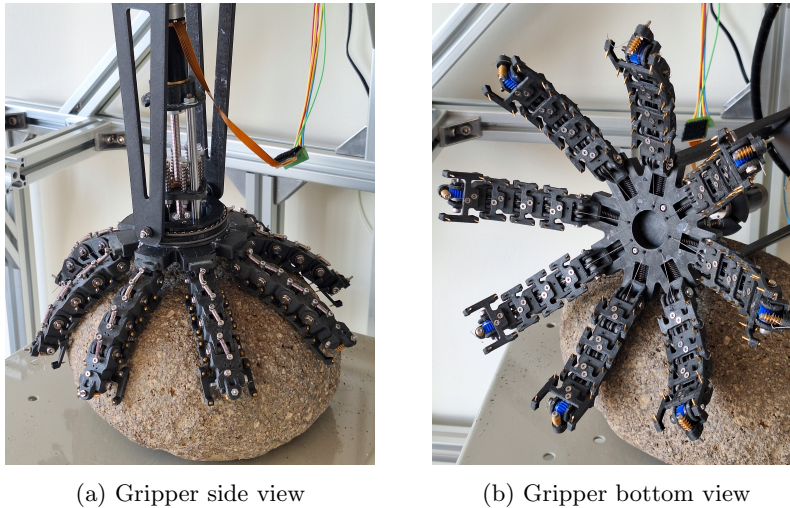


Fig. 2: Gripper prototype

## 2.1 Principle

To offer the advantages of soft gripping in space environments, the proposed gripping system relies on multiple tendon-driven fingers divided into 4 phalanges. The tether is attached to the extremity of the finger and is guided through a series of pulleys connected to each joint of the finger, as shown in Fig. 3. This architecture was previously used in the softgripper developed by Hirose [11], which shows great results in matching irregular shapes. Each phalanx is identical in length  $l$  and shape to provide a modular option for longer or shorter fingers. The aim of Hirose's research was to generate uniform pressure along the contact areas of the fingers by adjusting the diameter ratio between two consecutive pulleys, which allowed a controlled and gentle grasping of the target. In the case of grasping rocky targets, a more power-oriented approach was taken. When grasping a convex-shaped target, the fingertips generate more resistive force against the detachment motion, as the friction force orientation is normal to the target surface. When using the same diameter of the pulleys along the whole finger, the pressure applied to the target during grasping is distributed toward the fingertip, increasing the efficiency of the gripper. The pressure distribution can be derived from the equations presented in [11]. In the case of a series of identical pulleys, the torque  $\tau$  created by the tether tension  $T$  is constant for each joints of the finger and can be expressed as

$$\tau = r \times T \quad (1)$$

with  $r$  the radius of the pulley.

Considering that the torque  $\tau$  in each joint is constant, the pressure  $p_{j+1}$  applied by phalanx  $j$  can be derived as

$$p_{j+1} = \frac{\tau}{L_j} \quad (2)$$

where  $L_i$  is defined as

$$L_j = \begin{cases} \sum_{p=0}^{n-1-j} \left( \sum_{m=0}^p l_{n-m} \right) l_{n-p} & j = 0 \sim n-1 \\ 0 & j = n \end{cases} \quad (3)$$

When the lengths  $l$  of all the phalanx are equal, Eq.2 can be simplified to

$$\forall j \in [0, n] \quad p_{j+1} = \frac{2\tau}{l^2[(n-j)(n+1-j)]} \quad (4)$$

For the gripper presented in this study, each finger is composed of  $n = 4$  phalanges. The pressure distribution for each phalanx can then be expressed as

$$p_1 = \frac{\tau}{10l^2} \quad p_2 = \frac{\tau}{6l^2} \quad p_3 = \frac{\tau}{3l^2} \quad p_4 = \frac{\tau}{l^2} . \quad (5)$$

The pressure is distributed along the finger, with the maximum value at the fingertip. For each phalanx, it is equally divided between the spines in contact

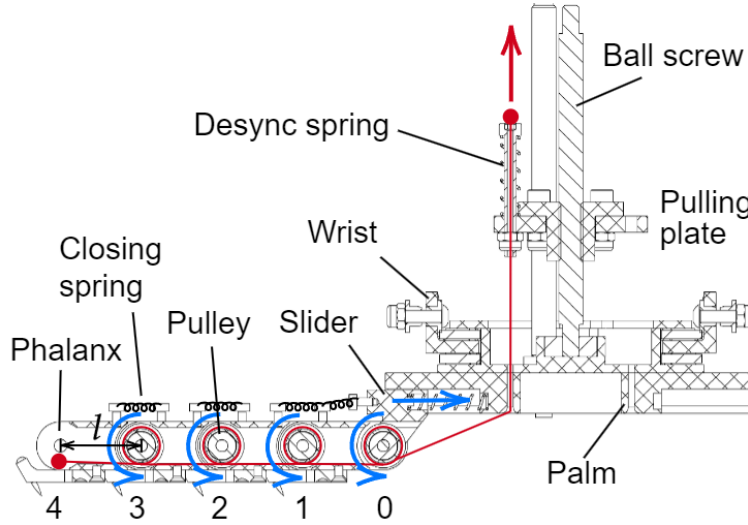


Fig. 3: Section view of the gripping system

with the target. The total pressure increases as the length between each joint  $l$  is reduced and the number of joints increases. However, physical limitations such as spine attachment, assembly and maintenance, pulley radius, and overall gripper diameter dictated the dimensions.

## 2.2 Actuation

When designing embedded systems and effectors for mobile robotics, it is important to take into account energy efficiency. Gripping mechanisms may require a continuous supply of current to maintain the grasp on the target. Therefore, the gripper actuation has been designed with a self locking feature utilizing a ball screw with a pitch of 1mm. The ball screw creates the linear motion that pulls the tethers to close the fingers with the help of a 5W DC brushless motor. The high level of reduction provided by the ball screw prevents back drive in the system. As long as the motor does not rotate to relieve tension on the tethers, the pulling plate is locked, and the fingers continue to apply pressure on their target.

In the softgripper design [11], the opening of the gripper was controlled using a secondary motor and tether. In this study, the opening action is passively ensured using tension springs placed between each phalanx. Although this solution adds resistance against the closing action of the gripper, it simplifies the overall architecture to a single actuator and one tether per finger. This allows for a lighter and more compact design.

The challenge with having a single actuator for multiple tethers is that every finger will be synchronously closing and opening at the same rate. For a linear

displacement  $\Delta z$  of the ball screw nut, each tether will be pulled by the same displacement  $\Delta z$ . This goes against the goal of soft gripping, where all fingers must be free to individually adapt to the target shape. To counteract this, a desync spring, shown in Fig. 3 was integrated into the actuation chain. This allows each finger to move independently of the other fingers. To account for each finger  $i$  needing their own displacement  $\Delta z_i$ , each tether is attached to the pulling plate using a hollowed screw and a compression spring. During the closing motion, if finger  $i$  is locked in position to target, the hollowed screw will sink into the pulling plate and continue its motion at a depth of  $h_i = \Delta z - \Delta z_i$ . The tether tension  $T_i$  will increase at a rate of  $T_i = k_{spring} \times h_i$ , but finger  $i$  will not prevent the pulling plate from moving further. The grasping motion of the target is completed when the equilibrium between the sum of the tensions of each tether  $T_i$  and the targeted motor torque  $\tau_{motor}$  is reached. This solution is a simple and effective way for the gripper to adapt to a random shape, although it comes at the cost of small disparities in the pressure applied by each of the fingers onto the target.

### 2.3 Microspines for rock grasping

The use of small sharp spines, referred to as microspines, has been proven to be effective in securing a good grip on the rough surface of rocks [6–8, 19]. As shown in Fig. 4, microspines latch onto the surface asperities and produce a counteracting friction force  $f_k$  directed against the detachment motion of the gripper. Following the method presented in [7], such asperities can be modeled as a triangular projection with a slope angle  $\beta$ , and the local friction coefficient  $\mu'$  of a microspine can be expressed as follows.

$$\mu' = \frac{\mu + \tan \beta}{1 - \mu \tan \beta} \quad (6)$$

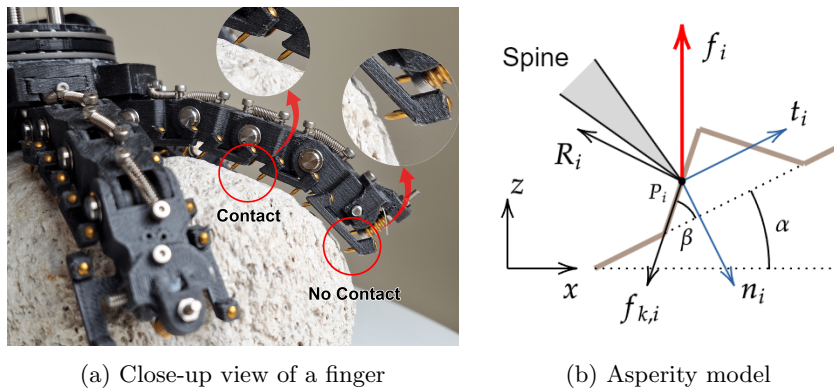


Fig. 4: Spine interaction with a rocky surface

Section 2.1 explained that pulling the control cord creates pressure on the target surface. This pressure, represented locally in Fig. 4b as  $n_i$ , is applied at a single contact point  $P_i$  perpendicularly to the local surface of the target, modeled here as a slope of angle  $\alpha$ . The reaction force  $R_i$  can be expressed as:

$$R_i = n_i \cos \beta \quad (7)$$

Given the total detachment force  $F$ , the local detachment force  $f_i$  is distributed along the spines that are in contact with the target. The slipping condition can be written as:

$$f_i < f_{k_i} = \mu' R_i \sin(\alpha + \beta) \quad (8)$$

With only the normal pressure  $n_i$ , the friction force  $f_{k_i}$  is sensible to the slope angles  $\alpha$  and  $\beta$ , and does not guarantee that the microspine will connect with favorably matching asperities. For this reason, a tangential force acting on the base of the finger has been implemented. The base of each finger is linked to the palm via a sliding part as shown in Fig. 3, with its degree of freedom along the radial axis of the gripper. Equation 7 can be rewritten as follows.

$$R_i = n_i \cos \beta + t_i \sin(\beta) \quad (9)$$

The total friction force generated by a spine  $i$  of a phalanx  $j$  for a finger  $a$  with  $n_a$  spines in contact with a convex target can be expressed as follows.

$$f_{k_i} = \mu' \left( \frac{r \times T}{L_j} \cos \beta + \frac{T}{n_a} \sin \beta \right) \sin(\alpha + \beta) \quad (10)$$

With  $r$  the radius of the pulley and  $T$  the tension of the finger tether.

### 3 Performance evaluation

A novel gripping system has been introduced that provides the benefits of soft gripping for extreme environments while including microspines technology for gripping rocks in space. The performances of the gripper have been assessed through different experiments conducted on a testing bench and will be presented in this section.

#### 3.1 Test environment

Gripping performance can be characterized by the amount of force that the gripper can withstand before detaching from the target. In the case of climbing robots, the orientation of the detachment force varies greatly depending on the inclination of the slope or cliff being climbed. The force can be a constant load over a long period of time or can be impulse shaped due to the motion of the robot. For the purpose of assessing the gripping performances under a wide range of parameters, a testing bench, presented in Fig. 5 was developed.

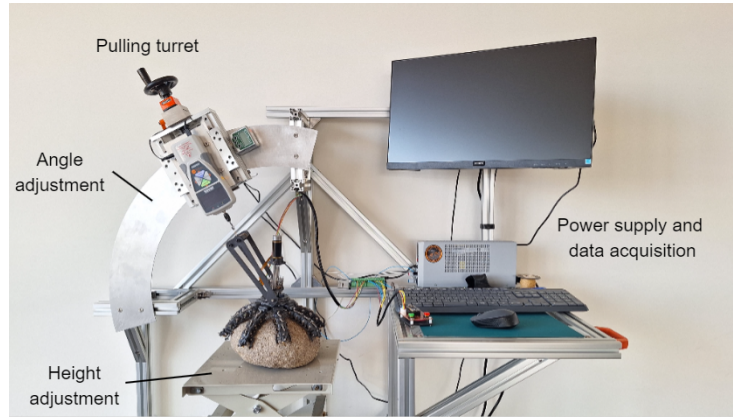


Fig. 5: Gripper grasping a basalt rock on the testing bench

The testing bench is composed of a manually actuated pulling turret on which is attached a force meter with a resolution of 0.01 N and a acquisition frequency of 0.1 s. The turret is mounted on a curved rail to adjust the angle of the pulling action from a range of  $0^\circ$  to  $90^\circ$  that can be dialed with a  $0.1^\circ$  precision using an absolute digital inclinometer. The axial displacement of the turret is measured through a graduated analog display with a resolution of 0.01 mm. The target is bolted to a height-adjustable platform used to calibrate the gripper wrist joint to align with the center of the radius of the curved rail. The wrist of the gripper is a universal joint with roll and yaw freedom, allowing the detachment force to be applied at the center of the gripper regardless of the force orientation.

### 3.2 Gripping performances experiments

The gripper was tested using multiple random-shaped rocks of different sizes (Fig.6a), but the unevenness of the shape hinders the repeatable aspect of the tests. In order to observe the gripper performances in a wide but controllable range, experiments were conducted on a set of spherical targets covered in #40 grit sandpaper (Fig. 6b). The curvature diameters of the targets were derived from the diameter of the gripper  $D = 270$  mm as follows.

$$D_1 = \frac{D}{2} = 135mm \quad D_2 = D = 270mm \quad D_3 = \frac{3D}{2} = 405mm \quad (11)$$

To assess the impact of the configuration and geometry of the microspines, three types of spine interface (Fig. 6c) were designed and tested. The number of spines varies from two to four spines per module with an inclination of  $15^\circ$  or  $30^\circ$ .

Performances were evaluated by measuring the maximum force required to detach the gripper from its target. The force was applied using the pulling turret and measured with the force meter. This experiment was conducted from a

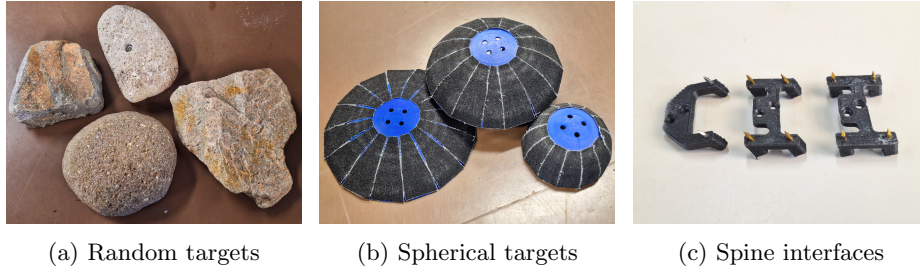


Fig. 6: Targets and spine interfaces used for the experiment

pulling angle range of  $0^\circ$  to  $90^\circ$  with increments of  $10^\circ$  on each target, with each spine configuration repeated 5 times.

A complementary study on gripper behavior was conducted with an increase in load over time. The motor actuation power was tested in the range of 0.15 A to 0.275 A, creating, respectively, 84 mN m and 179 mN m torque on the ball screw, in increments of 0.025 A.

## 4 Results and discussion

In this section, the results of the experiments will be showcased. After multiple gripping tests on random-shaped rocks (Fig. 6a), the gripping performances averaged at around 35.68 N with a standard deviation of 17.33 N.

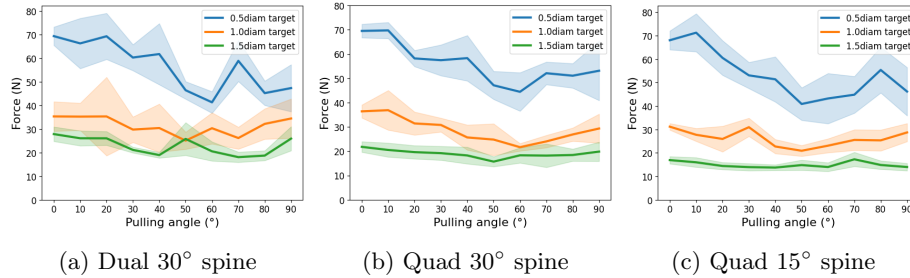


Fig. 7: Target curvature impact on performances with standard deviation

In the results shown in Figs. 7 and 8, the variation in gripping performance can be observed. As expected, the gripping force increases as the target diameter decreases as a result of the orientation of the resistive friction force. As the pulling angle increases from  $0^\circ$ , a decrease in performance is observed, followed by an increase around the  $80^\circ$  mark. This behavior can be attributed to how each finger contributes against the detachment motion. At  $0^\circ$ , all fingers contribute equally to oppose the pulling force. As the angle increases, the strain shifts to

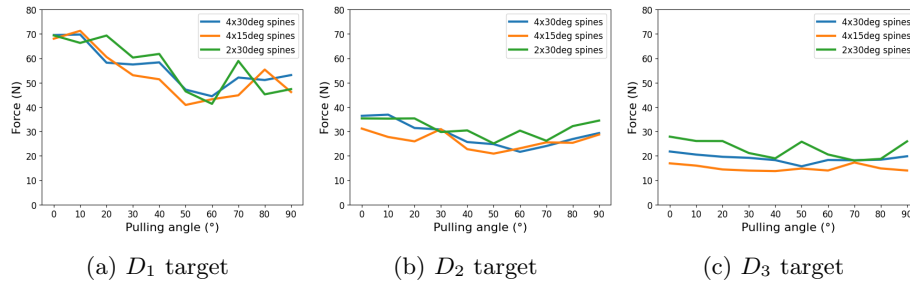


Fig. 8: Spine configuration impact on gripping performances

the opposite side of the detachment, resulting in the opposite fingers carrying more load than the others. This causes imbalance in the gripping action and increases the chances of slipping. As the angle approaches  $90^\circ$ , the opposite side fingers generate a strong resistive force in complete opposition to the detachment motion, therefore increasing the performances.

In Fig. 8, the impact of spine configuration on gripping performance is presented. The results show that while all configurations follow the same tendency as explained in the previous paragraph, a  $30^\circ$  inclination spine fares better overall. This behavior is attributed to the difficulty of the lower-angle spine to secure itself onto a suitable asperity before or after slipping. The number of spines also shows variations in performance. The dual spine configuration seems to hold the highest maximum detachment force, although the standard deviation in Fig. 7 show a slightly larger variance than the quad spine configurations. The distribution of the finger phalanx pressure onto fewer contact points helps the finger to match the shape of the target and apply a stronger local force, but may be more vulnerable to slipping or poor asperity contact.

Finally, experiments were conducted on the gripper behavior under increasing load and on the effect of motor torque on gripping performance. The results in Fig.9 demonstrate the slipping action that occurs during gripping. A linear continuous increase in gripping force can be observed until around 20N, prior to which the gripper provided a secure and immobile anchor on the target. Then, slipping begins to occur as shown by the sharp drop in gripping force. The first slip does not detach the gripper from the target, but weakens the maximum performances in some cases. In other cases, the slip allows fingers with underperforming contacts to attach to a more suitable area, increasing the maximum performance beyond the first slip limit. The ability of the gripper to recover from slipping mainly lies in the tether tension and torque applied by the actuator. As shown in Fig. 9a, not enough tension or too much tension can hinder the ability of the slipping spines to latch onto another asperity. For the current gripper prototype, an optimal actuation power between 0.225 A and 0.25 A generates the best gripping performance (Fig.9b).

In the case of a 20 kg legged robot such as SCAR-E, to climb on the ceiling of a lunar cave using a tripod gait, the maximum force required can be estimated

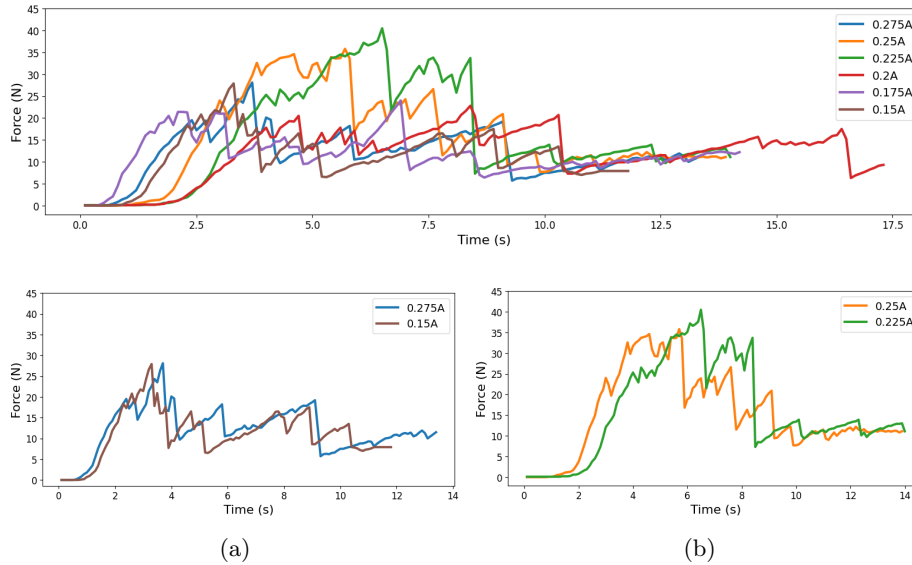


Fig. 9: Gripping performances over time with different actuator current

at around 10.8 N per gripper. On Mars, the force required for a similar task is around 24.73 N. Looking at the experimental results, the gripper is able to provide a reliable gripping action in this range and can be considered a suitable system for climbing in lunar, martian or microgravity environment.

Further tests will be conducted on the gripper, including the measure of the pressure distribution at each phalanx. The spine interface will be improved to provide more compliance with uneven surfaces and better adherence to the target surface.

## 5 Conclusion

Despite technological advances in prehension technologies for robotic systems, applications in space remain challenging due to the harshness of the environment. This study aims to develop a novel gripping system for space robots to allow grasping and climbing on rocky terrain such as asteroid surfaces or Moon caves. The gripper aims to combine soft gripping technology to optimize the contact with the target and microspine gripping to latch on rough rocky surface. Its design revolves around the creation of rotation and translation motion of compliant fingers with a single actuator to provide adaptability to the target shape and strong adhesion to its surface.

The gripping performance was evaluated using multiple parameters, such as the pulling angle, the target shape, the spine configuration, and the actuation power. The gripper is able to provide a reliable anchor for 1R space exploration legged robot such as SCAR-E in reduced gravity environment.

## References

1. Hein, A. M., Matheson, R. & Fries, D. A techno-economic analysis of asteroid mining. *Acta Astronautica* **168**, 104–115. ISSN: 0094-5765 (2020).
2. Gao, Y., Su, B., Jiang, L. & Gao, F. Multi-legged robots: progress and challenges. *National Science Review* **10**, nwac214. ISSN: 2095-5138 (Oct. 2022).
3. Tedeschi, F. & Carbone, G. Design Issues for Hexapod Walking Robots. *Robotics* **3**, 181–206. ISSN: 2218-6581 (2014).
4. Conroy, M. *FSI rover classification details* 2022. <https://fsi.ucf.edu/student-design/robotics/roverclassification/>.
5. Wagner, R. V. & Robinson, M. S. Lunar Pit Morphology: Implications for Exploration. *Journal of Geophysical Research: Planets* **127**, e2022JE007328 (2022).
6. Parness, A. *et al.* Gravity-independent Rock-climbing Robot and a Sample Acquisition Tool with Microspine Grippers. *Journal of Field Robotics* **30**, 897–915 (2013).
7. Nagaoka, K. *et al.* Passive Spine Gripper for Free-Climbing Robot in Extreme Terrain. *IEEE Robotics and Automation Letters* **3**, 1765–1770 (2018).
8. Li, X. *et al.* An Underactuated Adaptive Microspines Gripper for Rough Wall. *Biomimetics* **8** (2023).
9. Newill-Smith, D., Trieu, T., Boohene, A. N. & Stengel, R. F. Prototype for an Asteroid Exploratory Robot Using Multi-Phalanx Microspine Grippers. *AIAA SPACE 2015 Conference and Exposition* (2015).
10. Zhou, J., Chen, S. & Wang, Z. A Soft-Robotic Gripper With Enhanced Object Adaptation and Grasping Reliability. *IEEE Robotics and Automation Letters* **2**, 2287–2293 (2017).
11. Hirose, S. & Umetani, Y. The development of soft gripper for the versatile robot hand. *Mechanism and Machine Theory* **13**, 351–359. ISSN: 0094-114X (1978).
12. Tadakuma, K. *et al.* Fire-Resistant Deformable Soft Gripper Based on Wire Jamming Mechanism in *2020 3rd IEEE International Conference on Soft Robotics (RoboSoft)* (2020), 740–747.
13. Liu, C.-H. *et al.* Optimal Design of a Soft Robotic Gripper for Grasping Unknown Objects. *Soft Robotics* **5**, 452–465 (2018).
14. Hu, Q., Dong, E. & Sun, D. Soft Gripper Design Based on the Integration of Flat Dry Adhesive, Soft Actuator, and Microspine. *IEEE Transactions on Robotics* **37**, 1065–1080 (2021).
15. Glick, P. *et al.* A Soft Robotic Gripper With Gecko-Inspired Adhesive. *IEEE Robotics and Automation Letters* **3**, 903–910 (2018).
16. Nishida, T., Shigehisa, D., Kawashima, N. & Tadakuma, K. *Development of universal jamming gripper with a force feedback mechanism* in *2014 Joint 7th International Conference on Soft Computing and Intelligent Systems (SCIS)* (2014), 242–246.
17. Amend, J. R., Brown, E., Rodenberg, N., Jaeger, H. M. & Lipson, H. A Positive Pressure Universal Gripper Based on the Jamming of Granular Material. *IEEE Transactions on Robotics* **28**, 341–350 (2012).
18. Spenko, M. Making Contact: A Review of Robotic Attachment Mechanisms for Extraterrestrial Applications. *Advanced Intelligent Systems* **5**, 2100063 (2023).
19. Asbeck, A. T., Kim, S., Cutkosky, M. R., Provancher, W. R. & Lanzetta, M. *Scaling hard vertical surfaces with compliant microspine arrays* in *Proceedings of Robotics: Science and Systems* (Cambridge, USA, 2005).